

REGULAR PAPER

Signal corrector and decoupling estimations for UAV control

X. Wang 

University of Nottingham, Aerospace Engineering, Nottingham, United Kingdom
Email: wangxinhua04@gmail.com

Received: 27 May 2022; **Revised:** 15 September 2022; **Accepted:** 28 September 2022

Keywords: Large-error sensing; Uncertainty; Signal corrector; Decoupling estimation

Abstract

For a class of uncertain systems with large-error sensing, the low-order stable signal corrector and observer are presented for signal correction and uncertainty estimation according to completely decoupling estimation. The model-free signal corrector can reject the bounded stochastic disturbance/error in global position sensing, and system uncertainty can be estimated by the observer, even the existence of large disturbance in position sensing. Furthermore, a general form of signal corrector is given. The describing function method is used to analyse the robustness of the corrector in frequency domain, and the parameter selection rules are presented. The merits of the signal corrector includes its model free, gain-bounded stable structure, sufficient rejection of bounded stochastic disturbance/error in sensing and ease of parameters' regulation. The corrector and observer are applied to a UAV navigation and control for large disturbance/error corrections in position/attitude angle and the uncertainties estimation in the UAV flight dynamics. The control laws are designed according to the correction-estimation results. Finally, experiments demonstrate the effectiveness of the proposed method.

Nomenclature

x_1	system variable
x_2	system variable
x_3	system extended variable
$h(t)$	unknown function in system
$\sigma(t)$	system uncertainty
$c_\sigma(t)$	unknown derivative of $\sigma(t)$
L_σ	upper bound of $c_\sigma(t)$
y_{o1}	position measurement
y_{o2}	velocity measurement
$d(t)$	bounded disturbance in position
$n_1(t)$	high frequency noise in position
$n_2(t)$	high frequency noise in velocity
L_d	upper bound of $d(t)$
\hat{x}_1	corrector variable
\hat{x}_2	corrector variable
\hat{x}_3	observer variable
\hat{x}_4	observer variable
ω_{nc}	natural frequency of corrector
ω_{no}	natural frequency of observer
k_1	corrector parameter

k_2	corrector parameter
k_3	observer parameter
k_4	observer parameter
ε_c	perturbation parameter in corrector
ε_o	perturbation parameter in observer
α_c	function power in corrector
α_o	function power in observer
m	mass of UAV
g	gravity acceleration
l	rotor distance to gravity centre
x	position in x-direction
y	position in y-direction
z	position in z-direction
ψ	yaw angle
θ	pitch angle
ϕ	roll angle
J_ϕ	moment of inertia about roll
J_θ	moment of inertia about pitch
J_ψ	moment of inertia about yaw
b	rotor force coefficient
k	rotor torque coefficient
Δ_x	uncertainty in x-direction
Δ_y	uncertainty in y-direction
Δ_z	uncertainty in z-direction
Δ_ψ	uncertainty in yaw
Δ_θ	uncertainty in pitch
Δ_ϕ	uncertainty in roll
k_x	drag coefficient in x-direction
k_y	drag coefficient in y-direction
k_z	drag coefficient in z-direction
k_ψ	drag coefficient in yaw
k_θ	drag coefficient in pitch
k_ϕ	drag coefficient in roll
F_i	thrust force by rotor i
Q_i	reactive torque of rotor i
ω_i	rotor i rotational velocity

1. Introduction

Usually UAV flight needs information of position, attitude and dynamic model. Global position plays very important roles for large-range navigation and control [1, 2]. Meanwhile, the uncertainties exist in UAV flight dynamics: aerodynamic disturbance, unmodelled dynamics and parametric uncertainties are inevitable. These uncertainties bring serious challenges for control system design.

GPS (Global positioning system) can provide position information with accuracy of several meters or even tens of meters [3, 4]. Also, the adverse circumstances may contaminate signals from GPS [4]. Velocity is also necessary for UAV navigation and control. GPS can measure device velocity with two different accuracies: (1) large-error velocity by the difference method with accuracy of a meter per second due to GPS position accuracy and noise effect; (2) precise velocity by Doppler shift measurement with accuracy of a few centimeters even millimeters per second [5, 6]. Alternatively, accurate velocity of device can be measured by a Doppler radar sensor [7]. Except for sensing, velocity can be estimated from position using robust observers [8–13]. However, the relatively accurate measurements of position are required for these observer, and position with stochastic disturbance brings much worse velocity estimation.

Without position and velocity sensing, INS (inertial navigation system) can estimate them through integrations from acceleration measurement. However, even small measurement error or very weak non-zero mean noise in acceleration through integrations can cause velocity and position to drift over time. The observer-based INS methods were used to estimate unknown variables in navigation [14, 15]. However, position signals are limited to be local and bounded, but not global.

For attitude information, an IMU (inertial measurement unit) can determine the attitude angles from the measured angular rates through integration, and angle drifts happen. Meanwhile, the outputs of the accelerometers and the magnetometer in IMU can determine the large-error pitch, roll and yaw angles [16].

In order to reduce the disturbances/errors in position/attitude angle, KF (Kalman filter) or EKF (extended Kalman filter) is adopted for signals fusion to restrict the defects of individual measurements based on the optimisation of a recursive least mean square error [17–19]. Thus, the accuracy of system outputs is improved. For KF/EKF, the relatively accurate system models are needed. Moreover, existence of uncertainty in noise statistics limits the KF/EKF parameters' regulation. In addition, for EKF, system model linearisation may cause filter divergence, and the derivation of the Jacobian matrices are nontrivial.

The uncertainties or disturbances in system can be estimated by the extended state observers [8, 11, 20–22]. However, the accurate position measurements are required as these observer inputs. Even the accurate velocity is used for uncertainty estimation, the disturbance in position cannot be corrected.

In this paper, a class of uncertain systems with large disturbance/error in position measurement are considered. As an example, the relevant problems in UAV navigation and control are also considered. According to the relations between position, velocity and uncertainty in system, as well as the large disturbance/error in position sensing and the relatively accurate measurement in velocity, the position correction and uncertainty estimation are completely decoupled. The independent signal corrector and uncertainty observer are presented according to finite-time stability [23, 24] and the complete decoupling estimation. In the stable signal corrector, the bounded stochastic disturbance in position sensing can be reduced by the accurate velocity measurement. With the specific nonlinear functions and the perturbation parameter, the corrector can reduce the disturbance/error in sensing further. Moreover, the bounded system gains can avoid peaking phenomenon for the corrector. Importantly, through estimation decoupling, the observer can estimate the system uncertainty using the accurate velocity measurement independently, avoiding the use of large-error position information. Both corrector and observer are the low-order systems, their system parameters are regulated easily. Frequency analysis is used to explain the robustness of the corrector and observer.

The signal corrector and uncertainty observer are applied to an experiment on a quadrotor UAV navigation and control, and the performance is compared to the traditional KF-based navigation [25]. In the experiment, the following adverse conditions are considered: large stochastic disturbances/errors in GPS position/IMU attitude angles, uncertainties in position/attitude dynamics, and existence of high-frequency noise. The signal correctors are adopted to correct the disturbances/errors in GPS position/IMU attitude angles, and the observers are used to estimate the uncertainties in the UAV dynamics. Finally, the control laws based on the correction and estimation are formed to stabilize the UAV flight.

Comparing with the existing related studies, the contributions of this paper include:

(1) *Completely decoupling estimation*: The completely decoupling estimation is implemented for a class of systems with large stochastic disturbance in position sensing and system uncertainty. Thus, using the same accurate velocity measurement but towards the opposite directions, the presented signal corrector can correct the stochastic disturbance in position sensing, and the system uncertainty is estimated by the uncertainty observer. However, the usual observers cannot correct the disturbance/error in position sensing, and the positions are taken as the input for estimation. It brings the large estimation errors, even it makes the system unstable.

(2) *Relax requirements for system model and sensing disturbance*: For the uncertain systems with large stochastic disturbance in position sensing, the presented method does not need the accurate models and complete noise statistics information. Only the upper bounds of the stochastic disturbance in sensing and system uncertainty are required. The design of the signal corrector is model free, and only two measurement signals in position and velocity are required for the correction. The design of the observer is based on partial system model. For KF/EKF, the relatively accurate system model and noise statistics are necessary, and the parameters' regulation and estimation performance are affected adversely by uncertainties in system model and noise statistics.

(3) *High-precision correction/estimation and strong robustness*: The signals fusion in the corrector is implemented according to the finite-time stability with strong robustness against bounded disturbance. With the use of specific continuous nonlinear functions, and due to the strong robustness against bounded stochastic disturbance, the correction error is small enough even for large disturbance. In addition, through frequency analysis, the design corrector and observer have the ability of low-pass filters. Therefore, the corrector and observer provide the accurate and smoothed correction/estimation outputs.

(4) *Ease of parameters' regulation*: The implementation of completely decoupling estimation makes both corrector and observer in low order. For the stability, the parameters' selection is only required to be satisfied with a Routh–Hurwitz Stability Criterion. For improving the robustness, the power of the nonlinear function in the corrector is regulated.

(5) *Suitable to the complex and adverse dynamic systems*: The corrector and observer can be applied to the complex flight dynamic systems: relatively accurate navigation and control are implemented even large stochastic disturbances/errors in position/attitude sensing and existence of modelling uncertainties/disturbances.

2. Problem description

The technical problems considered in this paper for a class of uncertain systems with large-error sensing include:

(1) large bounded stochastic error/disturbance in position sensing; (2) existence of system uncertainty; (3) overshoot/oscillations existence and difficult parameters selection in high-order estimation systems.

2.1 Correction of large error in position and estimation of uncertainty in position dynamics

Measurement conditions: GPS provides the large error/disturbance position of device, and the relatively accurate velocity can be determined by GPS with Doppler shift measurement or by a Doppler radar sensor. Also, the uncertainties/disturbances exist in system dynamics. Under these conditions, we have:

Question 1: How to correct the bounded stochastic error/disturbance in position and to estimate uncertainty in position dynamics?

2.2 Correction of large error in attitude angle and estimation of uncertainty in attitude dynamics

Measurement conditions: The gyroscopes in IMU provide the direct measurement of relatively accurate angular rate. The large-error attitude angles can be determined by the outputs of the accelerometer and magnetometer in IMU. Then:

Question 2: How to correct the bounded error/disturbance in attitude angle and to estimate uncertainty in attitude dynamics?

2.3 Difficult parameters selection and oscillations existence for high-order estimation system

For multivariate estimation/correction, a high-order observer can be used. However, many system parameters need to be adjusted cooperatively, and oscillations are prone to occur. The oscillations can amplify the noise in the estimation outputs. Therefore, we hope the decoupling low-order estimate systems can be designed to overcome these issues instead of a single high-order observer.

3. General form of decoupling corrector and observer for uncertain systems with large error sensing

3.1 Uncertain system with large error/disturbance sensing

The following uncertain system has a minimum number of states and inputs, but it retains the features that is considered for many applications:

$$\begin{aligned} \dot{x}_1 &= x_2 \\ \dot{x}_2 &= h(t) + \sigma(t) \\ y_{o1} &= x_1 + d(t) \\ y_{o2} &= x_2 + n(t), \end{aligned} \tag{1}$$

where, x_1 and x_2 are the states; $h(t) \in \mathfrak{R}$ is the known function including the controller and the other unknown terms; $\sigma(t) \in \mathfrak{R}$ is the system uncertainty; y_{o1} and y_{o2} are the sensing outputs; $d(t)$ is the unknown bounded stochastic error/disturbance in measurement, it may be in the low, intermediate or high frequency bands, and $\sup_{t \in [0, \infty)} |d(t)| \leq L_d < +\infty$; $n(t)$ is the high-frequency noise. The design missions include: error correction in y_{o1} ; estimation of $\sigma(t)$.

3.2 System extension

Assumption 3.1. Suppose uncertainty $\sigma(t)$ in system (1) satisfies

$$\dot{\sigma}(t) = c_\sigma(t), \tag{2}$$

where, $c_\sigma(t)$ is unknown and bounded, and $\sup_{t \in [0, \infty)} |c_\sigma(t)| \leq L_\sigma < +\infty$. Actually, this assumption holds for many applications, e.g., crosswind dynamics.

In system (1), in order to estimate the uncertainty $\sigma(t)$, we define it as a new variable, i.e., $x_3 = \sigma(t)$. Therefore, $\dot{x}_3 = \dot{\sigma}(t) = c_\sigma(t)$ holds. Then, second-order system (1) is extended equivalently into a third-order system, i.e.,

$$\begin{aligned} \dot{x}_1 &= x_2 \\ \dot{x}_2 &= x_3 + h(t) \\ \dot{x}_3 &= c_\sigma(t) \\ y_{o1} &= x_1 + d(t) \\ y_{o2} &= x_2 + n(t). \end{aligned} \tag{3}$$

3.3 System decoupling according to the accurate measurement

The estimations of x_1 and x_3 are in the opposite directions from the relatively accurate measurement y_{o2} . Then, system (3) can be decoupled into the following two systems:

(1) the unobservable (from y_{o2}) system

$$\begin{aligned} \dot{x}_1 &= x_2 \\ y_{o1} &= x_1 + d(t) \\ y_{o2} &= x_2 + n(t). \end{aligned} \tag{4}$$

(2) and the observable system

$$\begin{aligned} \dot{x}_2 &= x_3 + h(t) \\ \dot{x}_3 &= c_\sigma(t) \\ y_{o2} &= x_2 + n(t). \end{aligned} \tag{5}$$

3.4 General form of completely decoupling correction and estimation

We give the following assumptions before the correction and estimation systems are constructed.

Assumption 3.2. *Suppose the origin is the finite-time-stable equilibrium of system*

$$\begin{aligned} \dot{z}_1 &= z_2 \\ \dot{z}_2 &= f_c(z_1, k \cdot z_2), \end{aligned} \tag{6}$$

where, $f_c(\cdot)$ is continuous and $f_c(0, 0) = 0$, and $k > 1$.

Assumption 3.3. *For (6), there exist $\rho \in (0, 1]$ and a nonnegative constant a such that*

$$|f_c(\tilde{z}_1, k \cdot z_2) - f_c(\bar{z}_1, k \cdot z_2)| \leq a |\tilde{z}_1 - \bar{z}_1|^\rho, \tag{7}$$

where, $\tilde{z}_1, \bar{z}_1 \in \mathfrak{R}$.

Remark 3.1. There are many types of functions satisfying this assumption. For example, one such function is $|\tilde{x}^\rho - \bar{x}^\rho| \leq 2^{1-\rho} |\tilde{x} - \bar{x}|^\rho$, $\rho \in (0, 1]$.

Assumption 3.4. *Suppose the origin is the finite-time-stable equilibrium of system*

$$\begin{aligned} \dot{z}_3 &= z_4 + f_{o1}(z_3) \\ \dot{z}_4 &= f_{o2}(z_3), \end{aligned} \tag{8}$$

where, $f_{o1}(\cdot)$ and $f_{o2}(\cdot)$ are continuous, and $f_{o1}(0) = 0$ and $f_{o2}(0) = 0$.

Usually high-frequency noise does not determine (but affects) system stability. Thus, the noise $n(t)$ is ignored when we consider the system stability. When considering the system robustness in frequency analysis, we will analyze the effect of noise $n(t)$.

Theorem 3.1 *(General form of decoupling signal corrector and uncertainty observer):*

The following uncertain system, for which Assumptions 3.1~3.4 hold, is considered:

$$\begin{aligned} \dot{x}_1 &= x_2 \\ \dot{x}_2 &= h(t) + \sigma(t) \\ y_{o1} &= x_1 + d(t) \\ y_{o2} &= x_2, \end{aligned} \tag{9}$$

where, x_1 and x_2 are the states; $h(t) \in \mathfrak{R}$ is the known function including the controller; $\sigma(t) \in \mathfrak{R}$ is the system uncertainty, $\dot{\sigma}(t) = c_\sigma(t)$, and $c_\sigma(t)$ is bounded with $\sup_{t \in [0, \infty)} |c_\sigma(t)| \leq L_\sigma < +\infty$; y_{o1} and y_{o2} are the measurement outputs; $d(t)$ is the bounded stochastic disturbance/error in measurement y_{o1} , and $\sup_{t \in [0, \infty)} |d(t)| \leq L_d < +\infty$. In order to correct large error in measurement y_{o1} and to estimate uncertainty $\sigma(t)$ (i.e., x_3), the completely decoupling second-order corrector and observer are designed, respectively, as follows:

(1) Signal corrector

$$\begin{aligned} \hat{x}_1 &= \hat{x}_2 \\ \varepsilon_c^3 \hat{x}_2 &= f_c(\varepsilon_c(\hat{x}_1 - y_{o1}), \hat{x}_2 - y_{o2}), \end{aligned} \tag{10}$$

where, $\varepsilon_c \in (0, 1)$; and

(2) Uncertainty observer

$$\begin{aligned} \varepsilon_o \hat{x}_3 &= \varepsilon_o \hat{x}_4 + f_{o1}(\hat{x}_3 - y_{o2}) + \varepsilon_o h(t) \\ \varepsilon_o^2 \hat{x}_4 &= f_{o2}(\hat{x}_3 - y_{o2}), \end{aligned} \tag{11}$$

where, $\varepsilon_o \in (0, 1)$. Then, there exist $\gamma_c > \frac{3}{\rho}$, $\gamma_o > 1$ and $t_s > 0$, such that, for $t \geq t_s$,

$$\begin{aligned} \hat{x}_1 - x_1 &= O(\varepsilon_c^{\rho\gamma_c-1}); \hat{x}_2 - x_2 = O(\varepsilon_c^{\rho\gamma_c-2}); \\ \hat{x}_3 - x_2 &= O(\varepsilon_c^{2\gamma_o}); \hat{x}_4 - \sigma(t) = O(\varepsilon_c^{2\gamma_o-1}), \end{aligned} \tag{12}$$

where, $O(\varepsilon_c^{\rho\gamma_c-1})$ means that the error between \hat{x}_1 and x_1 is of order $O(\varepsilon_c^{\rho\gamma_c-1})$ [26]. The proof of Theorem 3.1 is presented in the Appendix.

Remark 3.2. In the signal corrector (10), the input signals include the measurements y_{o1} and y_{o2} , and the states \hat{x}_1 and \hat{x}_2 estimate the system states x_1 and x_2 , respectively. Importantly, the bounded stochastic disturbance/error $d(t)$ in measurement y_{o1} is rejected. In the observer (11), the input signal is the measurement y_{o2} , and \hat{x}_3 and \hat{x}_4 estimate x_2 and uncertainty $\sigma(t)$, respectively. Two independent low-order estimation systems are designed to correct the large error in measurement and to estimate the uncertainty, and the completely decoupling estimations are implemented.

4. Implementation of completely decoupling corrector and observer for uncertain systems

In the following, we implement: For a class of uncertain systems with bounded stochastic error/disturbance sensing, the completely decoupling low-order corrector and observer are designed to implement signal correction and uncertainty estimation, respectively.

4.1 Design of decoupling low-order corrector and observer for uncertain system with large-error sensing

Theorem 4.1: *The following uncertain system is considered:*

$$\begin{aligned} \dot{x}_1 &= x_2 \\ \dot{x}_2 &= h(t) + \sigma(t) \\ y_{o1} &= x_1 + d(t) \\ y_{o2} &= x_2, \end{aligned} \tag{13}$$

where, x_1 and x_2 are the states; $h(t) \in \mathfrak{R}$ is the known function including the controller; $\sigma(t) \in \mathfrak{R}$ is the system uncertainty, $\dot{\sigma}(t) = c_\sigma(t)$, and $c_\sigma(t)$ is bounded with $\sup_{t \in [0, \infty)} |c_\sigma(t)| \leq L_\sigma < +\infty$; y_{o1} and y_{o2} are the measurement outputs; $d(t)$ is the bounded stochastic disturbance/error in measurement y_{o1} , and $\sup_{t \in [0, \infty)} |d(t)| \leq L_d < +\infty$. In order to correct large error in measurement y_{o1} and to estimate uncertainty $\sigma(t)$, the completely decoupling second-order corrector and observer are designed, respectively, as follows:

(1) Signal corrector

$$\begin{aligned} \hat{x}_1 &= \hat{x}_2 \\ \varepsilon_c^3 \hat{x}_2 &= -k_1 |\varepsilon_c(\hat{x}_1 - y_{o1})|^{\frac{\alpha_c}{2-\alpha_c}} \text{sign}(\hat{x}_1 - y_{o1}) - k_2 |\hat{x}_2 - y_{o2}|^{\alpha_c} \text{sign}(\hat{x}_2 - y_{o2}), \end{aligned} \tag{14}$$

where, $k_1 > 0, k_2 > 0, \alpha_c \in (0, 1)$, and time-scale parameter $\varepsilon_c \in (0, 1)$; and

(2) Uncertainty observer

$$\begin{aligned} \varepsilon_o \hat{x}_3 &= \varepsilon_o \hat{x}_4 - k_4 |\hat{x}_3 - y_{o2}|^{\frac{\alpha_o+1}{2}} \text{sign}(\hat{x}_3 - y_{o2}) + \varepsilon_o h(t) \\ \varepsilon_o^2 \hat{x}_4 &= -k_3 |\hat{x}_3 - y_{o2}|^{\alpha_o} \text{sign}(\hat{x}_3 - y_{o2}), \end{aligned} \tag{15}$$

where, $k_3 > 0, k_4 > 0, \alpha_o \in (0, 1)$, and time-scale parameter $\varepsilon_o \in (0, 1)$. Then, there exist $\gamma_c > \frac{6-3\alpha_c}{\alpha_c}, \gamma_o > 1$ and $t_s > 0$, such that, for $t \geq t_s$,

$$\begin{aligned} \hat{x}_1 - x_1 &= O\left(\varepsilon_c^{\frac{\alpha_c}{2-\alpha_c} \gamma_c - 1}\right); \hat{x}_2 - x_2 = O\left(\varepsilon_c^{\frac{\alpha_c}{2-\alpha_c} \gamma_c - 2}\right); \\ \hat{x}_3 - x_2 &= O\left(\varepsilon_c^{2\gamma_o}\right); \hat{x}_4 - \sigma(t) = O\left(\varepsilon_c^{2\gamma_o - 1}\right), \end{aligned} \tag{16}$$

where, $O\left(\varepsilon_c^{\frac{\alpha_c}{2-\alpha_c} \gamma_c - 1}\right)$ means that the error between \hat{x}_1 and x_1 is of order $O\left(\varepsilon_c^{\frac{\alpha_c}{2-\alpha_c} \gamma_c - 1}\right)$. The proof of Theorem 4.1 is presented in the Appendix.

4.2 Analysis of stability and robustness

Here, the describing function method is used to analyse the nonlinear behaviours of the corrector and observer. Although it is an approximation method, it inherits the desirable properties from the frequency response method for nonlinear systems. We will find that the corrector and observer lead to perform accurate estimation and strong rejection of noise under the condition of the bounded estimation gains.

In signal corrector (14) and uncertainty observer (15), for the nonlinear function $|*|^{\alpha_i} \text{sign}(*)$, by selecting $* = A_i \sin(\omega t)$, its describing function can be expressed by $N_i(A_i) = \frac{\Omega(\alpha_i)}{A_i^{1-\alpha_i}}$, where, $\Omega(\alpha_i) = \frac{2}{\pi} \int_0^\pi |\sin(\omega\tau)|^{\alpha_i+1} d\omega\tau$, and $\Omega(\alpha_i) \in [1, \frac{4}{\pi})$ when $\alpha_i \in (0, 1)$.

For the corrector (14), define: $\alpha_{c2} = \alpha_c \in (0, 1)$ and $\alpha_{c1} = \frac{\alpha_{c2}}{2 - \alpha_{c2}}$; $\hat{x}_1 - y_{o1} = A_{c1} \sin(\omega t)$ and $\hat{x}_2 - y_{o2} = A_{c2} \sin(\omega t)$. Here, A_{c1} is the error magnitude in position sensing, and A_{c2} is the error magnitude in velocity sensing. Therefore, the approximations of signal corrector (14) and uncertainty observer (15) through the describing function method are given, respectively, by

$$\begin{aligned} \hat{x}_1 &= \hat{x}_2 \\ \varepsilon^3 \hat{x}_2 &= -\frac{k_1 \Omega(\alpha_{c1})}{A_{c1}^{1-\alpha_{c1}}} \varepsilon (\hat{x}_1 - y_{o1}) - \frac{k_2 \Omega(\alpha_{c2})}{A_{c2}^{1-\alpha_{c2}}} (\hat{x}_2 - y_{o2}), \end{aligned} \tag{17}$$

and

$$\begin{aligned} \hat{x}_3 &= \hat{x}_4 - \frac{k_4 \Omega\left(\frac{1+\alpha_o}{2}\right)}{\varepsilon_o A_o^{\frac{1-\alpha_o}{2}}} (\hat{x}_3 - y_{o2}) + h(t) \\ \hat{x}_4 &= -\frac{k_3 \Omega(\alpha_o)}{\varepsilon_o^2 A_o^{1-\alpha_o}} (\hat{x}_3 - y_{o2}). \end{aligned} \tag{18}$$

Define the Laplace transforms $\hat{X}_1(s) = L[\hat{x}_1], \hat{X}_2(s) = L[\hat{x}_2]$, and $Y_{o2}(s) = L[y_{o2}]$, for (17), the following transfer functions are determined:

$$\frac{\hat{X}_j(s)}{Y_{o2}(s)} = \frac{k_2 \frac{\Omega(\alpha_2)}{A_{c2}^{1-\alpha_2}} s^{j-1} + \varepsilon k_1 \frac{\Omega(\alpha_1)}{A_{c1}^{1-\alpha_1}} s^{j-2}}{\varepsilon^3 s^2 + k_2 \frac{\Omega(\alpha_2)}{A_{c2}^{1-\alpha_2}} s + \varepsilon k_1 \frac{\Omega(\alpha_1)}{A_{c1}^{1-\alpha_1}}}, \tag{19}$$

where, $j = 1, 2$. $\frac{\hat{X}_2(s)}{Y_{o2}(s)}$ means the velocity filtering output \hat{x}_2 ; and $\frac{\hat{X}_1(s)}{Y_{o2}(s)}$ means the effect of the corrector output \hat{x}_1 from the velocity measurement y_{o2} .

Table 1. Values of $\Omega(\alpha_{c2})$ and $\Omega(\alpha_{c1})$ with different α_{c2}

α_{c2}	$\Omega(\alpha_{c2})$	$\Omega(\alpha_{c1})$
0.8	1.0410	1.0712
0.5	1.1128	1.1596
0.3	1.1697	1.2093

We get the natural frequency of the corrector by

$$\omega_{nc} = \frac{\sqrt{k_1} \sqrt{\Omega(\alpha_1)}}{\varepsilon_c A_{c1} \frac{1 - \alpha_{c1}}{2}}, \tag{20}$$

and similarly the natural frequency of the observer is

$$\omega_{no} = \frac{\sqrt{k_3} \sqrt{\Omega(\alpha_o)}}{\varepsilon_o A_o \frac{1 - \alpha_o}{2}}. \tag{21}$$

The effects of the parameters on the corrector robustness are analysed as follows.

Frequency characteristic with different ε_c and α_{c2} . For the corrector, We select: $k_1 = 1, k_2 = 30; \alpha_{c2} = \alpha = 0.8, 0.5, 0.3; \varepsilon_c = \varepsilon = 0.8, 0.4, 0.25$, respectively. With different selections of α_{c2} , we get the other parameter values shown in Table 1.

The Bode plots of (19) with different ε_c and α_{c2} are presented in Fig. 1: Fig. 1(a) and (b) describe the frequency characteristics of $(y_{02} \rightarrow \hat{x}_2)$ and $(y_{02} \rightarrow \hat{x}_1)$, respectively.

Conclusions on the correction and estimation

From the proof of Theorem 1, the systems are finite time stable, and their approximations are asymptotically stable according to (17) and (18). According to the analysis in time and frequency domains, the system stability and robustness have the following properties:

(1) *Large error rejection in sensing:*

In time domain, from (16), in spite of the large error/disturbance in position sensing, the estimate errors are always small enough after a finite time. In addition, we find that even for unbounded position navigation, no drift exists in position due to the small bound of estimate errors. In frequency domain, from (20) and Fig. 1(a), when the error magnitude A_{c1} in position sensing is relatively large, the corrector natural frequency ω_{nc} is smaller, and much noise is rejected.

(2) *Strong correction from accurate y_{02} :*

From the system (13), we know that, $\dot{x}_1 = x_2$. According to Theorem 1, $\hat{x}_2 - y_{02} = \hat{x}_2 - x_2$ is small enough. Thus \hat{x}_2 approaches x_2 . According to $\hat{x}_1 = \hat{x}_2$ and system stability, the corrector output \hat{x}_1 approaches the actual position x_1 . Therefore, the large error/disturbance in position is corrected sufficiently. Furthermore, from the Bode plot of $\frac{\hat{X}_1(s)}{Y_{02}(s)}$ in Fig. 1(b), we find that, when y_{02} is in low frequency band, y_{02} contributes the correction very well, and the corrector output \hat{x}_1 approaches the integral of y_{02} ; while the noise in y_{02} is rejected in high frequency band.

(3) *No peaking (bounded gains of corrector):* If the large gains are selected, they make the bandwidth very large, and it is sensitive to high-frequency noise. Moreover, peaking phenomenon happens. It means that the maximal value of system output during the transient increases infinitely when the gains tend to infinity. For the presented corrector and observer, the system gains do not need to be large, and no peaking phenomenon happens. In fact, in the estimate errors, $\gamma_c > 1$ and $\gamma_o > 1$ are sufficiently large. Therefore, for any $\varepsilon_c \in (0, 1)$ and $\varepsilon_o \in (0, 1)$, the estimate errors are sufficiently small. Thus, ε_c and ε_o do not need small enough in the estimation systems. Meanwhile, from (17) and (18), near the neighborhood of equilibrium, $1/A_{c1}^{1-\alpha_{c1}}$ and $1/A_{c2}^{1-\alpha_{c2}}$ in the corrector and $1/A_o^{\frac{1-\alpha_o}{2}}$ in the observer are large enough,

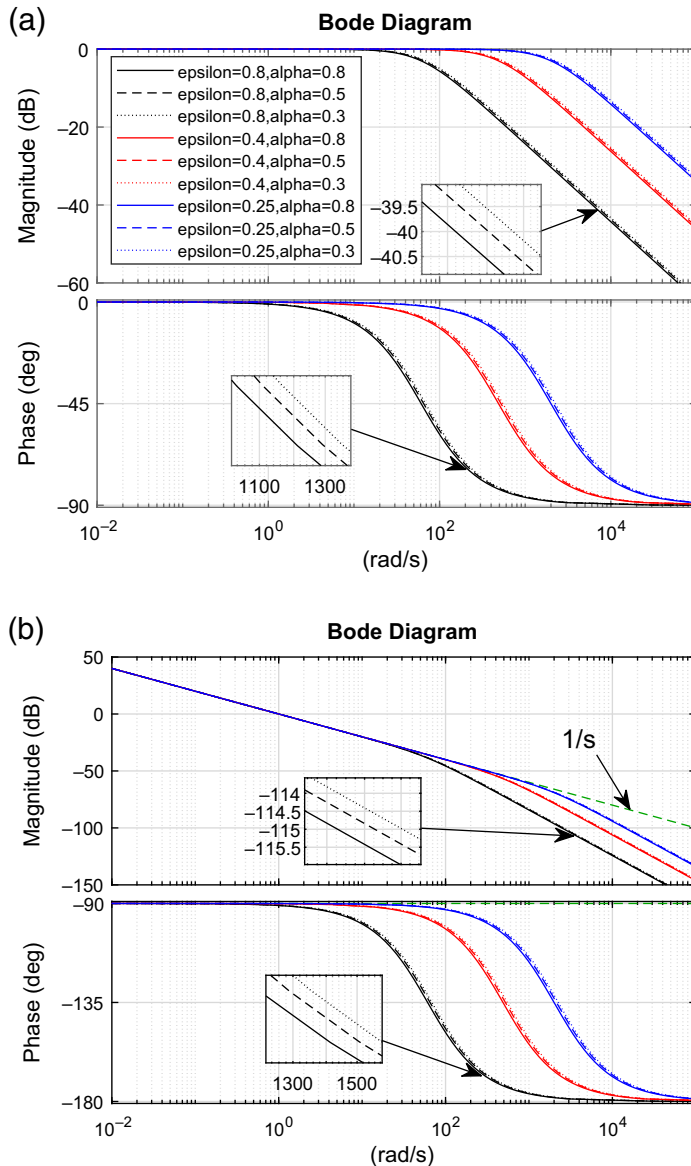


Figure 1. Bode plot of corrector with different parameter selections. (a) $y_{02} \rightarrow \hat{x}_2$ ($\epsilon = 0.8, 0.4, 0.25$; $\alpha = 0.8, 0.5, 0.3$). (b) $y_{02} \rightarrow \hat{x}_1$ ($\epsilon = 0.8, 0.4, 0.25$; $\alpha = 0.8, 0.5, 0.3$).

and these large terms make the feedback effect still strong. Therefore, the large parameter gains are unnecessary, and peaking is avoided.

(4) *No chattering*: Both corrector and observer are continuous, and their system outputs are smoothed. Therefore, the corrector and observer can provide smoothed estimations to reduce high-frequency chattering.

(5) *Robustness against noise*: If the errors magnitudes A_{c1} and A_o are relatively large, according to (20) and (21), the natural frequencies ω_{nc} and ω_{no} for the corrector and observer are relatively small. Thus, more disturbances/errors are rejected, and A_{c1} and A_o become small. Furthermore, the corrector and observer are continuous, and the estimate outputs are smoothed. Therefore, the high-frequency noise in the estimations is rejected.

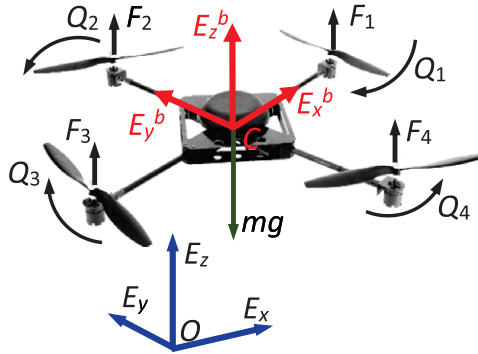


Figure 2. Forces and torques of quadrotor UAV.

(6) *Performance by parameter selections:* ε_c affects the frequency bandwidth: Decreasing ε_c , the frequency bandwidth becomes larger; increasing ε_c , the frequency bandwidth becomes smaller, and much noise is rejected. $\alpha_{c2} \in (0, 1)$ affects the estimate precision: smaller $\alpha_{c2} \in (0, 1)$ can obtain more precise estimations; on the other hand, relatively larger $\alpha_{c2} \in (0, 1)$ can reduce much noise.

4.3 Parameters selection rules of corrector and observer

Because the corrector and observer are completely decoupling, their parameters can be regulated independently. According to stability of nonlinear continuous systems [23], we have:

(1) *Parameters selection for system stability (Routh–Hurwitz Stability Criterion):*

Signal corrector (14): For any $\varepsilon_c \in (0, 1)$ and $\alpha_c \in (0, 1)$, $s^2 + \frac{k_2}{\varepsilon_c} s + k_1$ is Hurwitz if $k_1 > 0$ and $k_2 > 0$. Furthermore, in order to avoid oscillations, we select: $k_1 > 0$, $k_2 > 0$, $k_2^2 \geq 4\varepsilon_c^{4\alpha_c} k_1$, $\varepsilon_c \in (0, 1)$ and $\alpha_c \in (0, 1)$.

Uncertainty observer (15): $s^2 + k_4 s + k_3$ is Hurwitz if $k_3 > 0$ and $k_4 > 0$. Furthermore, in order to avoid oscillations, we select: $k_3 > 0$, $k_4 > 0$, and $k_4^2 \geq 4k_3$, $\varepsilon_o \in (0, 1)$ and $\alpha_o \in (0, 1)$.

Sensing error rejection: When the sensing error $d(t)$ in y_{o1} increases, i.e., L_d becomes larger, in order to reduce the error effect $k_1 L_d^{\frac{\alpha_c}{2-\alpha_c}}$ of $\delta_c = 2^{1-\frac{\alpha_c}{2-\alpha_c}} k_1 L_d^{\frac{\alpha_c}{2-\alpha_c}} + L_p$ in (64), parameter $k_1 > 0$ should decrease. Meanwhile, $\alpha_c \in (0, 1)$ can decrease to make $L_d^{\frac{\alpha_c}{2-\alpha_c}}$ smaller.

(2) *Parameters selection for filtering:*

ε_c (or ε_o) affects the frequency band of the corrector (or observer). If much noise exists, $\varepsilon_c \in (0, 1)$ (or $\varepsilon_o \in (0, 1)$) should increase, and/or $\alpha_c \in (0, 1)$ (or $\alpha_o \in (0, 1)$) increases, to make the low-pass frequency bandwidth narrow. Thus, noise can be rejected sufficiently. Also, from (20), k_1 decreases, the frequency band also decreases, and much noise will be rejected.

$\alpha_c \in (0, 1)$ (or $\alpha_o \in (0, 1)$) guarantees the finite-time stability of corrector (or observer), and it can avoid the selection of sufficiently small ε_c (or ε_o).

5. UAV navigation and control based on decoupling estimations

A UAV navigation and control with large-error sensing in position/attitude angle are considered. The UAV forces and torques are explained in Fig. 2, and the system parameters are introduced in Table 2.

Table 2. UAV parameters

Symbol	Quantity	Value
m	Mass of UAV	2.01kg
g	Gravity acceleration	9.81m/s ²
l	Rotor distance to gravity centre	0.2m
J_ϕ	Moment of inertia about roll	1.25kg · m ²
J_θ	Moment of inertia about pitch	1.25kg · m ²
J_ψ	Moment of inertia about yaw	2.5kg · m ²
b	Rotor force coefficient	2.923 × 10 ⁻³
k	Rotor torque coefficient	5 × 10 ⁻⁴

5.1 Quadrotor UAV dynamics

The inertial and fuselage frames are denoted by $\Xi_g = (E_x, E_y, E_z)$ and $\Xi_b = (E_x^b, E_y^b, E_z^b)$, respectively; ψ, θ and ϕ are the yaw, pitch and roll angles, respectively. $F_i = b\omega_i^2$ is the thrust force by rotor i , and its reactive torque is $Q_i = k\omega_i^2$. The sum of the four rotor thrusts is $F = \sum_{i=1}^4 F_i$. The motion equations of the UAV flight dynamics are expressed by

$$\ddot{x}_i = h_i(t) + \sigma_i(t), \tag{22}$$

where, $i = 1, \dots, 6$; $x_1 = x, x_2 = y, x_3 = z, x_4 = \psi, x_5 = \theta, x_6 = \phi$; $h_1(t) = \frac{u_x}{m}, h_2(t) = \frac{u_y}{m}, h_3(t) = \frac{u_z}{m} - g, h_4(t) = \frac{u_\psi}{J_\psi}, h_5(t) = \frac{u_\theta}{J_\theta}, h_6(t) = \frac{u_\phi}{J_\phi}$; $\sigma_1(t) = m^{-1}(-k_x \dot{x} + \Delta_x)$; $\sigma_2(t) = m^{-1}(-k_y \dot{y} + \Delta_y)$; $\sigma_3(t) = m^{-1}(-k_z \dot{z} + \Delta_z)$; $\sigma_4(t) = J_\psi^{-1}(-k_\psi \dot{\psi} + \Delta_\psi)$; $\sigma_5(t) = J_\theta^{-1}(-lk_\theta \dot{\theta} + \Delta_\theta)$; $\sigma_6(t) = J_\phi^{-1}(-lk_\phi \dot{\phi} + \Delta_\phi)$; $k_x, k_y, k_z, k_\psi, k_\theta$ and k_ϕ are the unknown drag coefficients; $(\Delta_x, \Delta_y, \Delta_z)$ and $(\Delta_\psi, \Delta_\theta, \Delta_\phi)$ are the uncertainties in position and attitude dynamics, respectively; $J = \text{diag}\{J_\psi, J_\theta, J_\phi\}$ is the matrix of three-axial moment of inertias; c_θ and s_θ are expressed for $\cos \theta$ and $\sin \theta$, respectively; and

$$\begin{aligned} u_x &= (c_\psi s_\theta c_\phi + s_\psi s_\phi)F, \quad u_y = (s_\psi s_\theta c_\phi - c_\psi s_\phi)F, \quad u_z = c_\theta c_\phi F, \\ u_\psi &= \frac{k}{b} \sum_{i=1}^4 (-1)^{i+1} F_i, \quad u_\theta = (F_3 - F_1)l, \quad u_\phi = (F_2 - F_4)l. \end{aligned} \tag{23}$$

5.2 Sensing

GPS provides the global position, and a microwave radar sensor measures velocity. An IMU gives the attitude angle and angular rate. The sensing outputs are:

$$y_{i,1} = x_i + d_i(t), \quad y_{i,2} = \dot{x}_i + n_i(t), \tag{24}$$

where, $d_i(t)$ is the bounded stochastic error/disturbance in sensing, and $\sup_{t \in [0, \infty)} |d_i(t)| \leq L_i < \infty$; $n_i(t)$ is the high-frequency noise; $i = 1, \dots, 6$.

The corrector (14) and observer (15) are used to estimate $(x, y, z, \psi, \theta, \phi)$ and the system uncertainties, respectively.

5.3 Control law design

The control laws are designed to stabilise the UAV flight. For the desired trajectory (x_d, y_d, z_d) and attitude angle $(\psi_d, \theta_d, \phi_d)$, the error systems of position and attitude dynamics can be expressed, respectively, by

$$\ddot{e}_p = m^{-1} (u_p + \Xi_p + \delta_p), \tag{25}$$

and

$$\ddot{e}_a = J^{-1}(u_a + \Xi_a + \delta_a), \tag{26}$$

where, $e_{p1} = x - x_d, e_{p2} = \dot{x} - \dot{x}_d, e_{p3} = y - y_d, e_{p4} = \dot{y} - \dot{y}_d, e_{p5} = z - z_d, e_{p6} = \dot{z} - \dot{z}_d; e_{a1} = \psi - \psi_d, e_{a2} = \dot{\psi} - \dot{\psi}_d, e_{a3} = \theta - \theta_d, e_{a4} = \dot{\theta} - \dot{\theta}_d, e_{a5} = \phi - \phi_d, e_{a6} = \dot{\phi} - \dot{\phi}_d;$

$$e_p = \begin{bmatrix} e_{p1} \\ e_{p3} \\ e_{p5} \end{bmatrix}, u_p = \begin{bmatrix} u_x \\ u_y \\ u_z \end{bmatrix}, \delta_p = \begin{bmatrix} \Delta_x - k_x \dot{x} \\ \Delta_y - k_y \dot{y} \\ \Delta_z - k_z \dot{z} \end{bmatrix}, \Xi_p = \begin{bmatrix} -m\ddot{x}_d \\ -m\ddot{y}_d \\ -m\ddot{z}_d - mg \end{bmatrix}, \tag{27}$$

and

$$e_a = \begin{bmatrix} e_{a1} \\ e_{a3} \\ e_{a5} \end{bmatrix}, u_a = \begin{bmatrix} u_\psi \\ u_\theta \\ u_\phi \end{bmatrix}, \Xi_a = \begin{bmatrix} -J_\psi \ddot{\psi}_d \\ -J_\theta \ddot{\theta}_d \\ -J_\phi \ddot{\phi}_d \end{bmatrix}, \delta_a = \begin{bmatrix} \Delta_\psi - k_\psi \dot{\psi} \\ \Delta_\theta - lk_\theta \dot{\theta} \\ \Delta_\phi - lk_\phi \dot{\phi} \end{bmatrix}. \tag{28}$$

5.3.1 Position dynamics control:

In the position dynamics, for the desired trajectory (x_d, y_d, z_d) , the control law

$$u_p = -\Xi_p - \hat{\delta}_p - m(k_{p1}\hat{e}_p + k_{p2}\dot{\hat{e}}_p), \tag{29}$$

is designed to make position error vectors $e_p \rightarrow \vec{0}$ and $\dot{e}_p \rightarrow \vec{0}$ as $t \rightarrow \infty$, where $\hat{e}_{p1} = \hat{x} - x_d, \hat{e}_{p2} = \hat{\dot{x}} - \dot{x}_d, \hat{e}_{p3} = \hat{y} - y_d, \hat{e}_{p4} = \hat{\dot{y}} - \dot{y}_d, \hat{e}_{p5} = \hat{z} - z_d, \hat{e}_{p6} = \hat{\dot{z}} - \dot{z}_d$ and $\hat{\delta}_p$ are estimated by the correctors; $k_{p1}, k_{p2} > 0$; and

$$\hat{e}_p = [\hat{e}_{p1} \hat{e}_{p3} \hat{e}_{p5}]^T, \dot{\hat{e}}_p = [\hat{e}_{p2} \hat{e}_{p4} \hat{e}_{p6}]^T. \tag{30}$$

5.3.2 Attitude dynamics control:

In the attitude dynamics, for the desired attitude angle $(\psi_d, \theta_d, \phi_d)$, the control law

$$u_a = -\Xi_a - \hat{\delta}_a - J(k_{a1}\hat{e}_a + k_{a2}\dot{\hat{e}}_a), \tag{31}$$

is designed to make attitude error vectors $e_a \rightarrow \vec{0}$ and $\dot{e}_a \rightarrow \vec{0}$ as $t \rightarrow \infty$, where, $\hat{e}_{a1} = \hat{\psi} - \psi_d, \hat{e}_{a2} = \hat{\dot{\psi}} - \dot{\psi}_d, \hat{e}_{a3} = \hat{\theta} - \theta_d, \hat{e}_{a4} = \hat{\dot{\theta}} - \dot{\theta}_d, \hat{e}_{a5} = \hat{\phi} - \phi_d, \hat{e}_{a6} = \hat{\dot{\phi}} - \dot{\phi}_d$ and $\hat{\delta}_a$ are estimated by the observers; $k_{a1}, k_{a2} > 0$; and

$$\hat{e}_a = [\hat{e}_{a1} \hat{e}_{a3} \hat{e}_{a5}]^T, \dot{\hat{e}}_a = [\hat{e}_{a2} \hat{e}_{a4} \hat{e}_{a6}]^T. \tag{32}$$

6. Experiment on uav navigation and control

In this section, a UAV flight experiment is presented to demonstrate the proposed method. The UAV flight platform is explained in Fig. 3. The UAV navigation and control based on the decoupling corrector and observer are implemented in the platform setup. The control system hardware is described in Fig. 4, whose elements include: A Gumstix and Arduino Mega 2560 (16MHz) are selected as the driven boards; Gumstix is to collect data from measurements; Arduino Mega is to run algorithm of estimation and control, and it sends out control commands; A XsensMTI AHRS (10kHz) provides the 3-axial accelerations, the angular rates and the earth’s magnetic field.

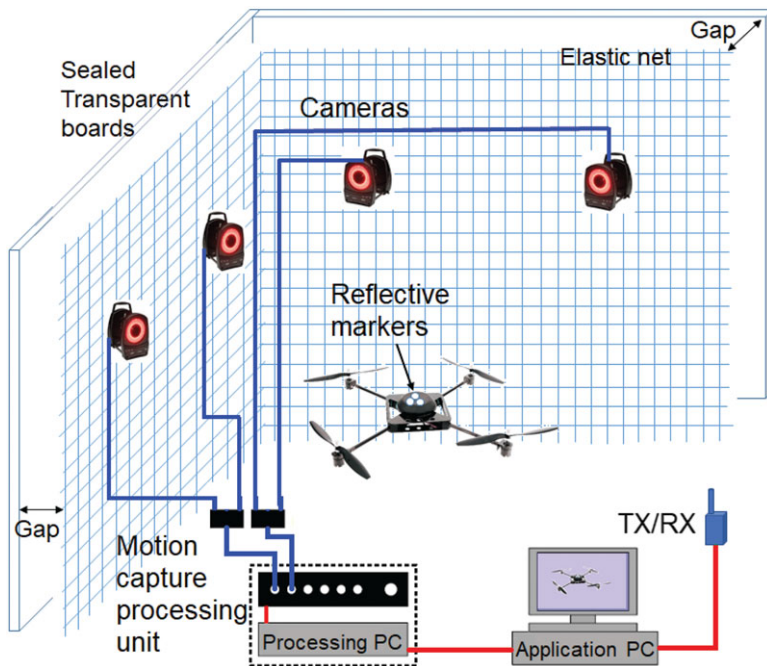


Figure 3. Platform of UAV flight control system.

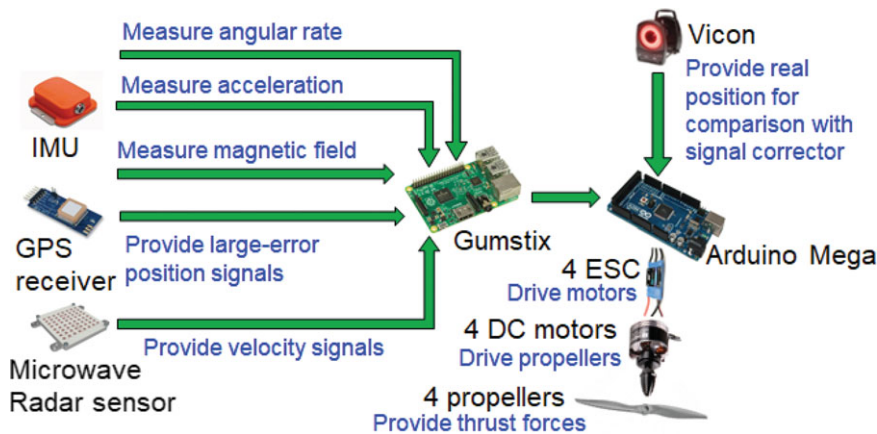


Figure 4. Control system hardware.

Real position acquisition for comparison: In order to get the real position for comparison with the estimation by the corrector, the output of the Vicon system with sub-millimeter accuracy is taken as the *real position*.

Large-error position from GPS: A low-cost GPS receiver provides intermittent position signals with accuracy of 10~20m. When an intermittence happens, the most recent valid readings from GPS are taken as the measured position signals.

Accurate velocity sensing: A 24GHz microwave Doppler radar sensor is adopted to measure the velocity.

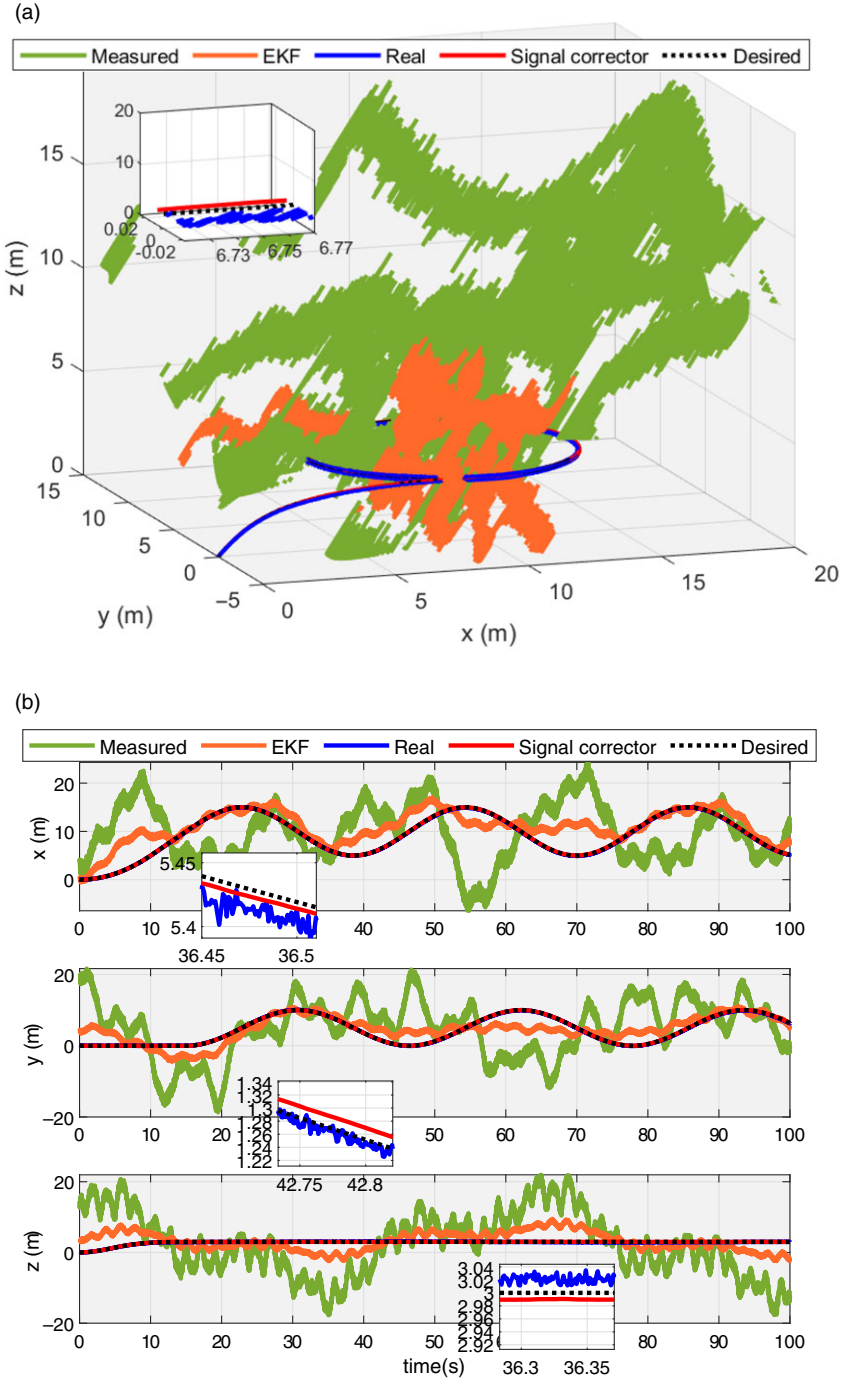


Figure 5. UAV navigation based on corrector and observer. (a) Navigation trajectories. (b) Position estimation.

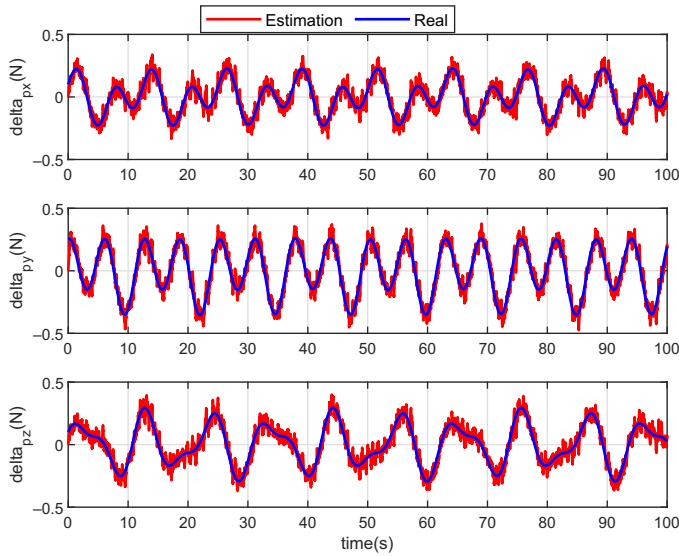


Figure 6. Uncertainty estimations.

Desired flight trajectory: The UAV desired trajectory includes: (1) take off and climb; (2) then fly in a circle with the radius of 5m, the velocity of 1m/s and the altitude of 3m. The 3D desired trajectory is shown in Fig. 5(a).

The corrected positions from the signal correctors and the uncertainty estimations from the observers are used in the controllers. Controllers (29) and (31) drive the UAV to track the desired trajectory. The corrector parameters: $k_{1,i} = 1, k_{2,i} = 30, 1/\varepsilon_{c,i} = 1.2, \alpha_{c,i} = 0.1, i = 1, 2, 3$. The observer parameters: $k_{3,i} = 20, k_{4,i} = 4, 1/\varepsilon_{o,i} = 1.1, \alpha_{o,i} = 0.6, i = 1, 2, 3$. The control law parameters: $k_{p1} = 2.5, k_{p2} = 4, k_{a1} = 2.5, k_{a2} = 4$. The position-correction performance of corrector is compared with the EKF-based GPS/radar sensor integration.

Figure 5(a) shows the comparison of flight trajectories in 3D space, including the measured from GPS, the real from the Vicon, the desired trajectories, and the estimations by the corrector and the EKF. Meanwhile, the trajectory comparisons in the three directions are shown in Fig. 5(b): The measurement errors in position from GPS are about 20m. The estimate errors by the corrector are less than 0.04m, while the estimate errors by the EKF are about 5m. Thus, the large errors/disturbances in position measurements are rejected by the corrector, and the effect of noises is reduced sufficiently. In addition, during a 1,000s-duration flight test, no drift happened.

Uncertainties estimation: The unexpected uncertainties exist in the UAV flight, and we cannot read these uncertainties. Therefore, the real uncertainties cannot be determined to compare with the estimate results. Here, we use a simulation to illustrate the uncertainty estimations by the observers. The unknown drag coefficients in the UAV model are supposed to be: $k_x = k_y = k_z = 0.01N \cdot s/m, k_\psi = k_\theta = k_\phi = 0.012N \cdot s/rad$. The unmodelled uncertainties are assumed as: $\Delta_x = 0.3 \sin(t) + 0.2 \cos(0.5t), \Delta_y = 0.2 \sin(0.5t) + 0.5 \cos(t), \Delta_z = 0.4 \sin(0.6t) + 0.2 \cos(t)$. Then, we can determine the *real uncertainty* vector δ_p according to (27). All the parameters in the system model, correctors, observers and controllers are selected the same as those in the above experiment. Figure 6 shows that the observers can get the accurate estimation of uncertainties although much noise exists.

7. Conclusions

For a class of uncertain systems with large-error sensing, according to the completely decoupling, the low-order signal corrector and observer have been developed to reject the large error in sensing and

to estimate the system uncertainty. The proposed corrector and observer have been demonstrated by a UAV navigation-control experiment: It succeeded in rejecting the large errors/disturbances in position sensing, and the system uncertainties were estimated accurately. It confirms the merits of the corrector and observer: They can provide accurate and smoothed estimation of position and uncertainty even simultaneous existence of large sensing error and system uncertainty.

References

- [1] Kwak, J. and Sung, Y. Autonomous UAV flight control for GPS-based navigation, *IEEE Access*, 2018, **6**, pp 37947–37955.
- [2] Grip, H.F., Fossen, T.I., Johansen, T.A. and Saberi, A. Globally exponentially stable attitude and gyro bias estimation with application to GNSS/INS integration, *Automatica*, 2015, **51**, pp 158–166.
- [3] Hsu, L.T. Analysis and modeling GPS NLOS effect in highly urbanized area, *GPS Solut.*, 2018, **22**, (7), pp 1–12.
- [4] Liu, Y.C., Bianchin, G. and Pasqualetti, F. Secure trajectory planning against undetectable spoofing attacks, *Automatica*, 2020, **112**, p 108655.
- [5] Freda, P., Angrisano, A., Gaglione, S. and Troisi, S. Time-differenced carrier phases technique for precise GNSS velocity estimation, *GPS Solut.*, 2015, **19**, pp 335–341.
- [6] Serrano, L., Kim, D., Langley, R.B., Itani, K. and Ueno, M. A GPS velocity sensor: How accurate can it be?. . . A first look, In *Proceedings of the 2004 National Technical Meeting of The Institute of Navigation*, 2004, San Diego, CA, pp 875–885.
- [7] Griffiths, H.D. *Small-and Short-Range Radar Systems GL Charvat*, CRC Press, Taylor & Francis Group, 6000 Broken Sound Parkway NW, Suite 300, Boca Raton, FL 33487-2742, USA. 2017. Distributed by Taylor & Francis Group, 2 Park Square, Milton Park, Abingdon, OX14 4RN, UK. xxvii; 385pp. Illustrated £ 77.99. (20% discount available to RAeS members via www.crcpress.com using AKQ07 promotion code). ISBN 978-1-138-07763-8. *Aeronaut. J.*, 2004, **123**, (1266), pp 1306–1306.
- [8] Levant, A. High-order sliding modes, differentiation and output-feedback control, *Int. J. Control*, 2003, **76**, (9/10), pp 924–941.
- [9] Levant, A. and Livne, M. Globally convergent differentiators with variable gains, *Int. J. Control*, 2018, **91**, pp 1994–2008.
- [10] Levant, A. and Yu, X. Sliding-mode-based differentiation and filtering, *IEEE Trans. Automat. Control*, 2018, **63**, (9), pp 3061–3067.
- [11] Khalil, H.K. Cascade high-gain observers in output feedback control, *Automatica*, 2017, **80**, pp 110–118.
- [12] Khalil, H.K. and Priess, S. Analysis of the use of low-pass filters with high-gain observers, *IFAC-PapersOnLine*, 2016, **49**, (18), pp 488–492.
- [13] Wang, X., Chen, Z. and Yang, G. Finite-time-convergent differentiator based on singular perturbation technique, *IEEE Trans. Automat. Control*, 2007, **52**, (9), pp 1731–1737.
- [14] Rogne, R.H., Bryne, T.H., Fossen, T.I. and Johansen, T.A. On the usage of low-cost mems sensors, strapdown inertial navigation, and nonlinear estimation techniques in dynamic positioning. *IEEE J. Ocean. Eng.*, 2020, **46**, (1), pp 24–39.
- [15] Hamel, T., Hua, M.D. and Samson, C. Deterministic observer design for vision-aided inertial navigation, In *2020 59th IEEE Conference on Decision and Control (CDC)*, December 2020, pp 1306–1313
- [16] Ludwig, S.A. and Jiménez, A.R. Optimisation of gyroscope and accelerometer/magnetometer portion of basic attitude and heading reference system, In *2018 IEEE International Symposium on Inertial Sensors and Systems (INERTIAL)*, 2018, Moltrasio, Italy, pp 1–4.
- [17] Deo, V.A., Silvestre, F. and Morales, M. Flight performance monitoring with optimal filtering applications, *Aeronaut. J.*, 2020, **124**, (1272), pp 170–188.
- [18] Lin, C.L., Li, J.C., Chiu, C.L., Wu, Y.W. and Jan, Y.W. Gyro-stellar inertial attitude estimation for satellite with high motion rate, *The Aeronautical Journal*, 2022, pp 1–15.
- [19] Stovner, B.N., Johansen, T.A., Fossen, T.I. and Schjø Iberg, I. Attitude estimation by multiplicative exogenous Kalman filter, *Automatica*, 2018, **95**, pp 347–355.
- [20] Wang, Y. and Zheng, X. Path following of Nano quad-rotors using a novel disturbance observer-enhanced dynamic inversion approach, *Aeronaut. J.*, 2019, **123**, (1266), p 11221134.
- [21] Liu, J., Vazquez, S., Wu, L., Marquez, A., Gao, H. and Franquelo, L.G. Extended state observer-based sliding-mode control for three-phase power converters, *IEEE Trans. Ind. Electron.*, 2017, **64**, (1), pp 22–31.
- [22] Wang, X.H., Chen, Z.Q. and Yuan, Z.Z. Output tracking based on extended observer for nonlinear uncertain systems. *Control Decis.*, 2004, **19**, (10), pp 1113–1116.
- [23] Bhat, S.P. and Bernstein, D.S. Geometric homogeneity with applications to finite-time stability, *Math. Control, Signals, Syst.*, 2005, **17**, (2), pp 101–127.
- [24] Bhat, S.P. and Bernstein, D.S. Finite-time stability of continuous autonomous systems, *Siam J. Control Optim.*, 2000, **38**, (3), pp 751–766.
- [25] Crassidis, J.L. Introduction to the special issue on the Kalman Filter and its aerospace applications, *J. Guid. Control Dyn.*, 2017, **40**, (9), pp 2137–2137.
- [26] Khalil, H.K. *Nonlinear Systems*, 3rd ed., Prentice-Hall, Englewood Cliffs, NJ, USA, 2002.
- [27] Wang, X. and Lin, H. Design and frequency analysis of continuous finite-time-convergent differentiator, *Aerosp. Sci. Technol.*, 2012, **18**, (1), pp 69–78.

A. Appendix

Proof of Theorem 3.1

Proof of the general signal corrector (10) in Theorem 3.1: Define the corrector error as $e_1 = \widehat{x}_1 - x_1$ and $e_2 = \widehat{x}_2 - x_2$. Then, the error system of signal corrector (10) and decoupled system (4) can be described by:

$$\begin{aligned} \dot{e}_1 &= e_2; \\ \varepsilon_c^3 \dot{e}_2 &= f_c(\varepsilon_c(e_1 - d(t)), e_2) - \varepsilon_c^3 \ddot{x}_2(t), \end{aligned} \tag{33}$$

and Equation (33) can be rewritten as

$$\begin{aligned} \frac{d\varepsilon_c e_1}{dt/\varepsilon_c} &= \varepsilon_c^2 e_2; \\ \frac{d\varepsilon_c^2 e_2}{dt/\varepsilon_c} &= f_c\left(\varepsilon_c e_1 - \varepsilon_c d(t), \frac{1}{\varepsilon_c^2} \varepsilon_c^2 e_2\right) - \varepsilon_c^3 \ddot{x}_2(t). \end{aligned} \tag{34}$$

By choosing the following coordinate transform

$$\tau_c = t/\varepsilon_c, z_1(\tau) = \varepsilon_c e_1, z_2(\tau_c) = \varepsilon_c^2 e_2, z_c = [z_1(\tau_c) \ z_2(\tau_c)]^T; \bar{d}(\tau) = \varepsilon_c d(t); \bar{p}(\tau) = \varepsilon_c^3 \ddot{x}_2(t), \tag{35}$$

we get $z_c = \Xi(\varepsilon_c)e_c$, where, $\Xi(\varepsilon_c) = \text{diag}\{\varepsilon_c, \varepsilon_c^2\}$ and $e_c = [e_1 \ e_2]^T$. It is rational the system acceleration is bounded, and we can assume that $|\ddot{x}_2(t)| \leq L_p < +\infty$. Then, (34) becomes

$$\begin{aligned} \frac{dz_1}{d\tau_c} &= z_2; \\ \frac{dz_2}{d\tau_c} &= f_c\left(z_1 - \bar{d}(\tau_c), \frac{1}{\varepsilon_c^2} z_2\right) - \bar{p}(\tau_c). \end{aligned} \tag{36}$$

Define $k = \frac{1}{\varepsilon_c^2}$ and

$$g(\tau_c, z_c(\tau_c)) = f_c\left(z_1 - \bar{d}(\tau_c), \frac{1}{\varepsilon_c^2} z_2\right) - f_c\left(z_1, \frac{1}{\varepsilon_c^2} z_2\right) - \bar{p}(\tau_c), \tag{37}$$

then, (36) can be rewritten as

$$\begin{aligned} \frac{dz_1}{d\tau_c} &= z_2; \\ \frac{dz_2}{d\tau_c} &= f_c(z_1, k \cdot z_2) + g(\tau_c, z_c(\tau_c)). \end{aligned} \tag{38}$$

From Assumption 3.3, the contraction mapping rule $\left|f_c\left(z_1 - \bar{d}(\tau_c), \frac{1}{\varepsilon_c^2} z_2\right) - f_c\left(z_1, \frac{1}{\varepsilon_c^2} z_2\right)\right| \leq a |\bar{d}(\tau_c)|^\rho$ holds, where, $\rho \in (0, 1]$. Then, we get

$$\delta \stackrel{\text{define}}{=} \sup_{(\tau_c, z_c) \in \mathbb{R}^3} |g(\tau_c, z_c(\tau_c))| \leq a |\varepsilon_c L_d|^\rho + \varepsilon_c^3 L_p \leq \varepsilon^\rho \delta_c, \tag{39}$$

where $\delta_c = aL_d^\rho + L_p$. From Assumption 3.2, the unperturbed system

$$\begin{aligned} \frac{dz_1}{d\tau_c} &= z_2; \\ \frac{dz_2}{d\tau_c} &= f(z_1, k \cdot z_2), \end{aligned} \tag{40}$$

is finite-time stable. Furthermore, from Proposition 8.1 in [23], Theorem 5.2 in [24] and (39), for (38), there exist the bounded constants $\mu_c > 0$ and $\Gamma(z_c(0)) > 0$, such that, for $\tau_c \geq \Gamma(z_c(0))$,

$$\|z_c(\tau)\| \leq \mu_c \delta^{\gamma_c} \leq \mu_c (\varepsilon_c^\rho \delta_c)^{\gamma_c}. \tag{41}$$

Therefore, from (35) and (41), we get

$$\| \varepsilon_c e_1 \varepsilon_c^2 e_2 \| \leq \mu_c (\varepsilon_c^\rho \delta_c)^{\gamma_c}, \tag{42}$$

for $t \geq \varepsilon_c \Gamma (\Xi(\varepsilon_c) e_c (0))$. Thus, for $\forall t \in [\varepsilon_c \Gamma (\Xi(\varepsilon_c) e_c (0)), \infty)$, the following relations hold:

$$|e_1| \leq L_c \varepsilon^{\rho \gamma_c - 1}, |e_2| \leq L_c \varepsilon^{\rho \gamma_c - 2}, \tag{43}$$

where, $L_c = \mu_c \delta_c^\gamma$. Then, (43) can be written as

$$e_1 = O(\varepsilon_c^{\rho \gamma_c - 1}), e_2 = O(\varepsilon_c^{\rho \gamma_c - 2}). \tag{44}$$

From Theorems 4.3 and 5.2 in [24], γ_c can be chosen to be arbitrarily large, and

$$\gamma_c > 3/\rho, \tag{45}$$

is not restrictive. Accordingly, we can get $\rho \gamma_c - i > 1$ for $i = 1, 2$. It implies that, for $\varepsilon_c \in (0, 1)$, the estimate error in (44) is of higher order than the small perturbation. Consequently, the corrector can make the estimate errors sufficiently small.

Proof of the general uncertainty observer (11) in Theorem 3.1:

The decoupled system (5) from (1) can be rewritten by

$$\begin{aligned} \varepsilon_o \dot{x}_2 &= \varepsilon_o x_3 + \varepsilon_o h(t) \\ \varepsilon_o^2 \dot{x}_3 &= \varepsilon_o^2 c_\sigma(t). \end{aligned} \tag{46}$$

Define the observer error as $e_3 = \widehat{x}_3 - x_2$ and $e_4 = \widehat{x}_4 - x_3$. Then, the error system of the observer (11) and the equivalent decoupled system (46) can be described by:

$$\begin{aligned} \varepsilon_o \dot{e}_3 &= \varepsilon_o e_4 + f_{o1}(e_3) \\ \varepsilon_o^2 \dot{e}_4 &= f_{o2}(e_3) - \varepsilon_o^2 c_\sigma(t), \end{aligned} \tag{47}$$

and Equation (47) can be rewritten as

$$\begin{aligned} \frac{de_3}{dt/\varepsilon_o} &= \varepsilon_o e_4 + f_{o1}(e_3) \\ \frac{d\varepsilon_o e_4}{dt/\varepsilon_o} &= f_{o2}(e_3) - \varepsilon_o^2 c_\sigma(t). \end{aligned} \tag{48}$$

By choosing the following coordinate transform

$$\tau_o = t/\varepsilon_o, z_3(\tau_o) = e_3, z_4(\tau_o) = \varepsilon_o e_4, z_o = [z_3(\tau_o) \ z_4(\tau_o)]^T; \bar{c}(\tau_o) = \varepsilon_o^2 c_\sigma(t), \tag{49}$$

we get $z_o = \Xi(\varepsilon_o) e_o$, where, $\Xi(\varepsilon_o) = \text{diag}\{1, \varepsilon_o\}$ and $e_o = [e_3 \ e_4]^T$. Then, (48) becomes

$$\begin{aligned} \frac{dz_3}{d\tau_o} &= z_4 + f_{o1}(z_3) \\ \frac{dz_4}{d\tau_o} &= f_{o2}(z_3) - \bar{c}(\tau_o). \end{aligned} \tag{50}$$

From (49), we can get

$$\delta_o \stackrel{\text{define}}{=} \sup_{\tau_o \in \mathbb{R}^+} |\bar{c}(\tau_o)| \leq \varepsilon_o^2 L_\sigma. \tag{51}$$

From Assumption 3.4, the unperturbed system

$$\begin{aligned} \frac{dz_3}{d\tau_o} &= z_4 + f_{o1}(z_3) \\ \frac{dz_4}{d\tau_o} &= f_{o2}(z_3), \end{aligned} \tag{52}$$

is finite-time stable. Furthermore, from Proposition 8.1 in [23], Theorem 5.2 in [24] and (51), for (50), there exist the bounded constants $\mu_o > 0$ and $\Gamma(z_o(0)) > 0$, such that, for $\tau_o \geq \Gamma(z_o(0))$,

$$\|z_o(\tau_o)\| \leq \mu_o \delta_o^{\gamma_o} \leq \mu_o (\varepsilon_o^2 L_o)^{\gamma_o}. \tag{53}$$

Therefore, from (49) and (53), we get

$$\|e_3 \varepsilon_o e_4\| \leq \mu_o (\varepsilon_o^2 L_o)^{\gamma_o}, \tag{54}$$

for $t \geq \varepsilon_o \Gamma(\Xi(\varepsilon_o)e_o(0))$. Thus, for $\forall t \in [\varepsilon_o \Gamma(\Xi(\varepsilon_o)e_o(0)), \infty)$, the following relations hold:

$$|e_3| \leq L_o \varepsilon_o^{2\gamma_o}, |e_4| \leq L_o \varepsilon_o^{2\gamma_o-1}, \tag{55}$$

where, $L_o = \mu_o L_o^{\gamma_o}$. Then, (55) can be written as

$$e_3 = O(\varepsilon_o^{2\gamma_o}), e_4 = O(\varepsilon_o^{2\gamma_o-1}). \tag{56}$$

From Theorems 4.3 and 5.2 in [24], γ_o can be chosen to be arbitrarily large, and

$$\gamma_o > 1, \tag{57}$$

is not restrictive. Accordingly, we can get $2\gamma_o - i > 1$ for $i = 0, 1$. It implies that, for $\varepsilon_o \in (0, 1)$, the estimate error in (56) is of higher order than the small perturbation. Consequently, the uncertainty observer can make the estimate errors sufficiently small.

Proof of Theorem 4.1

Proof of the signal corrector (14) in Theorem 4.1:

Define the corrector error as $e_1 = \widehat{x}_1 - x_1$ and $e_2 = \widehat{x}_2 - x_2$. Then, the error system of signal corrector (14) and decoupled system (4) can be described by:

$$\begin{aligned} \dot{e}_1 &= e_2; \\ \varepsilon_c^3 \dot{e}_2 &= -k_1 |\varepsilon_c(e_1 - d(t))|^{\frac{\alpha_c}{2-\alpha_c}} \text{sign}(e_1 - d(t)) - k_2 |e_2|^{\alpha_c} \text{sign}(e_2) - \varepsilon_c^3 \ddot{x}_2(t), \end{aligned} \tag{58}$$

and Equation (58) can be rewritten as

$$\begin{aligned} \frac{d\varepsilon_c e_1}{dt/\varepsilon_c} &= \varepsilon_c^2 e_2; \\ \frac{d\varepsilon_c^2 e_2}{dt/\varepsilon_c} &= -k_1 |\varepsilon_c e_1 - \varepsilon_c d(t)|^{\frac{\alpha_c}{2-\alpha_c}} \text{sign}(e_1 - d(t)) - \frac{k_2}{\varepsilon_c^{2\alpha_c}} |\varepsilon_c^2 e_2|^{\alpha_c} \text{sign}(e_2) - \varepsilon_c^3 \ddot{x}_2(t). \end{aligned} \tag{59}$$

By choosing the following coordinate transform

$$\tau_c = t/\varepsilon_c, z_1(\tau_c) = \varepsilon_c e_1, z_2(\tau_c) = \varepsilon_c^2 e_2, z_c = [z_1(\tau_c) \ z_2(\tau_c)]^T; \bar{d}(\tau_c) = \varepsilon_c d(t); \bar{p}(\tau_c) = \varepsilon_c^3 \ddot{x}_2(t), \tag{60}$$

we get $z_c = \Xi(\varepsilon_c)e_c$, where, $\Xi(\varepsilon_c) = \text{diag}\{\varepsilon_c, \varepsilon_c^2\}$ and $e_c = [e_1 \ e_2]^T$. Then, (59) becomes

$$\begin{aligned} \frac{dz_1}{d\tau_c} &= z_2; \\ \frac{dz_2}{d\tau_c} &= -k_1 |z_1 - \bar{d}(\tau_c)|^{\frac{\alpha_c}{2-\alpha_c}} \text{sign}(z_1 - \bar{d}(\tau_c)) - \frac{k_2}{\varepsilon_c^{2\alpha_c}} |z_2|^{\alpha_c} \text{sign}(z_2) - \bar{p}(\tau_c). \end{aligned} \tag{61}$$

Define

$$g(\tau_c, z(\tau_c)) = -k_1 \left\{ |z_1 - \bar{d}(\tau_c)|^{\frac{\alpha_c}{2-\alpha_c}} \text{sign}(z_1 - \bar{d}(\tau_c)) - |z_1|^{\frac{\alpha_c}{2-\alpha_c}} \text{sign}(z_1) \right\} - \bar{p}(\tau_c), \tag{62}$$

then, (61) can be rewritten as

$$\begin{aligned} \frac{dz_1}{d\tau_c} &= z_2; \\ \frac{dz_2}{d\tau_c} &= -k_1 |z_1|^{\frac{\alpha_c}{2-\alpha_c}} \text{sign}(z_1) - \frac{k_2}{\varepsilon_c^{2\alpha_c}} |z_2|^{\alpha_c} \text{sign}(z_2) + g(\tau_c, z(\tau_c)). \end{aligned} \tag{63}$$

Since the contraction mapping rule $|x^\rho - \bar{x}^\rho| \leq 2^{1-\rho} |x - \bar{x}|^\rho$, $\rho \in (0, 1]$, we obtain

$$\delta \stackrel{\text{define}}{=} \sup_{(\tau_c, z_c) \in \mathbb{R}^3} |g(\tau_c, z_c(\tau_c))| \leq 2^{1-\frac{\alpha_c}{2-\alpha_c}} k_1 L_d^{\frac{\alpha_c}{2-\alpha_c}} \varepsilon_c^{\frac{\alpha_c}{2-\alpha_c}} + \varepsilon_c^3 L_p \leq \varepsilon_c^{\frac{\alpha_c}{2-\alpha_c}} \delta_c, \tag{64}$$

where $\delta_c = 2^{1-\frac{\alpha_c}{2-\alpha_c}} k_1 L_d^{\frac{\alpha_c}{2-\alpha_c}} + L_p$. From [23], we know that the unperturbed system

$$\begin{aligned} \frac{dz_1}{d\tau_c} &= z_2; \\ \frac{dz_2}{d\tau_c} &= -k_1 |z_1|^{\frac{\alpha_c}{2-\alpha_c}} \text{sign}(z_1) - \frac{k_2}{\varepsilon_c^{2\alpha_c}} |z_2|^{\alpha_c} \text{sign}(z_2), \end{aligned} \tag{65}$$

is finite-time stable. Furthermore, from Proposition 8.1 in [23], Theorem 5.2 in [24] and (64), for (63), there exist the bounded constants $\mu_c > 0$ and $\Gamma(z_c(0)) > 0$, such that, for $\tau_c \geq \Gamma(z_c(0))$,

$$\|z_c(\tau_c)\| \leq \mu_c \delta_c^{\gamma_c} \leq \mu_c \left(\varepsilon_c^{\frac{\alpha_c}{2-\alpha_c}} \delta_c \right)^{\gamma_c}. \tag{66}$$

Therefore, from (60) and (66), we get

$$\|\varepsilon_c e_1 \varepsilon_c^2 e_2\| \leq \mu_c \left(\varepsilon_c^{\frac{\alpha_c}{2-\alpha_c}} \delta_c \right)^{\gamma_c}, \tag{67}$$

for $t \geq \varepsilon_c \Gamma(\Xi(\varepsilon_c)e_c(0))$. Thus, for $\forall t \in [\varepsilon_c \Gamma(\Xi(\varepsilon_c)e_c(0)), \infty)$, the following relations hold:

$$|e_1| \leq L_c \varepsilon_c^{\frac{\alpha_c}{2-\alpha_c} \gamma_c - 1}, |e_2| \leq L_c \varepsilon_c^{\frac{\alpha_c}{2-\alpha_c} \gamma_c - 2}, \tag{68}$$

where, $L_c = \mu_c \delta_c^{\gamma_c}$. Then, (68) can be written as

$$e_1 = O\left(\varepsilon^{\frac{\alpha_c}{2-\alpha_c} \gamma_c - 1}\right), e_2 = O\left(\varepsilon^{\frac{\alpha_c}{2-\alpha_c} \gamma_c - 2}\right). \tag{69}$$

From Theorems 4.3 and 5.2 in [24], γ_c can be chosen to be arbitrarily large, and

$$\gamma_c > \frac{6 - 3\alpha_c}{\alpha_c}, \tag{70}$$

is not restrictive. Accordingly, we can get $\frac{\alpha_c}{2-\alpha_c} \gamma_c - i > 1$ for $i = 1, 2$. It implies that, for $\varepsilon_c \in (0, 1)$, the estimate error in (69) is of higher order than the small perturbation. For $\varepsilon_c \in (0, 1)$, according to the Routh-Hurwitz Stability Criterion, $s^2 + \frac{k_2}{\varepsilon_c^{2\alpha_c}} s + k_1$ is Hurwitz if $k_1 > 0$ and $k_2 > 0$.

Proof of the uncertainty observer (15) in Theorem 4.1:

The decoupled system (5) from (1) can be rewritten by

$$\begin{aligned} \varepsilon_o \dot{x}_2 &= \varepsilon_o x_3 + \varepsilon_o h(t) \\ \varepsilon_o^2 \dot{x}_3 &= \varepsilon_o^2 c_\sigma(t). \end{aligned} \tag{71}$$

Define the observer error as $e_3 = \widehat{x}_3 - x_2$ and $e_4 = \widehat{x}_4 - x_3$. Then, the error system of observer (15) and decoupled system (71) can be described by:

$$\begin{aligned} \varepsilon_o \dot{e}_3 &= \varepsilon_o e_4 - k_4 |e_3|^{\frac{\alpha_o+1}{2}} \text{sign}(e_3) \\ \varepsilon_o^2 \dot{e}_4 &= -k_3 |e_3|^{\alpha_o} \text{sign}(e_3) - \varepsilon_o^2 c_\sigma(t), \end{aligned} \tag{72}$$

and Equation (72) can be rewritten as

$$\begin{aligned} \frac{de_3}{dt/\varepsilon_o} &= \varepsilon_o e_4 - k_4 |e_3|^{\frac{\alpha_o+1}{2}} \text{sign}(e_3) \\ \frac{d\varepsilon_o e_4}{dt/\varepsilon_o} &= -k_3 |e_3|^{\alpha_o} \text{sign}(e_3) - \varepsilon_o^2 c_\sigma(t). \end{aligned} \tag{73}$$

By choosing the following coordinate transform

$$\tau_o = t/\varepsilon_o, z_3(\tau_o) = e_3, z_4(\tau_o) = \varepsilon_o e_4, z_o = [z_3(\tau_o) \ z_4(\tau_o)]^T; \bar{c}(\tau_o) = \varepsilon_o^2 c_\sigma(t), \tag{74}$$

we get $z_o = \Xi(\varepsilon_o)e_o$, where, $\Xi(\varepsilon_o) = \text{diag}\{1, \varepsilon_o\}$ and $e_o = [e_3 \ e_4]^T$. Then, (73) becomes

$$\begin{aligned} \frac{dz_3}{d\tau_o} &= z_4 - k_4 |z_3|^{\frac{\alpha_o+1}{2}} \text{sign}(z_3) \\ \frac{dz_4}{d\tau_o} &= -k_3 |z_3|^{\alpha_o} \text{sign}(z_3) - \bar{c}(\tau_o). \end{aligned} \tag{75}$$

From (74), we can get

$$\delta_o \stackrel{\text{define}}{=} \sup_{\tau_o \in \mathcal{R}^+} |\bar{c}(\tau_o)| \leq \varepsilon_o^2 L_\sigma. \tag{76}$$

From Theorem 1 in [27], we know that the unperturbed system

$$\begin{aligned} \frac{dz_3}{d\tau_o} &= z_4 - k_4 |z_3|^{\frac{\alpha_o+1}{2}} \text{sign}(z_3), \\ \frac{dz_4}{d\tau_o} &= -k_3 |z_3|^{\alpha_o} \text{sign}(z_3), \end{aligned} \tag{77}$$

is finite-time stable. Furthermore, from Proposition 8.1 in [23], Theorem 5.2 in [24] and (76), for (75), there exist the bounded constants $\mu_o > 0$ and $\Gamma(z_o(0)) > 0$, such that, for $\tau_o \geq \Gamma(z_o(0))$,

$$\|z_o(\tau_o)\| \leq \mu_o \delta_o^{\gamma_o} \leq \mu_o (\varepsilon_o^2 L_\sigma)^{\gamma_o}. \tag{78}$$

Therefore, from (74) and (78), we get

$$\|e_3 \ \varepsilon_o e_4\| \leq \mu_o (\varepsilon_o^2 L_\sigma)^{\gamma_o}, \tag{79}$$

for $t \geq \varepsilon_o \Gamma(\Xi(\varepsilon_o)e_o(0))$. Thus, for $\forall t \in [\varepsilon_o \Gamma(\Xi(\varepsilon_o)e_o(0)), \infty)$, the following relations hold:

$$|e_3| \leq L_o \varepsilon_o^{2\gamma_o}, \quad |e_4| \leq L_o \varepsilon_o^{2\gamma_o-1}, \tag{80}$$

where, $L_o = \mu_o L_\sigma^{\gamma_o}$. Then, (80) can be written as

$$e_3 = O(\varepsilon_o^{2\gamma_o}), \quad e_4 = O(\varepsilon_o^{2\gamma_o-1}). \tag{81}$$

From Theorems 4.3 and 5.2 in [24], γ_o can be chosen to be arbitrarily large, and

$$\gamma_o > 1, \tag{82}$$

is not restrictive. Accordingly, we can get $2\gamma_o - i > 1$ for $i = 0, 1$. It implies that, for $\varepsilon_o \in (0, 1)$, the estimate error in (81) is of higher order than the small perturbation. According to the Routh-Hurwitz stability criterion, $s^2 + k_4 s + k_3$ is Hurwitz if $k_3 > 0$ and $k_4 > 0$.

This concludes the proof.